

Supporting Information for:

Plasmon Enhanced Catalysis-Driven Nanomotors with Autonomous Navigation for Deep Cancer Imaging and Enhanced Radiotherapy

Luntao Liu,^{‡ a} Qingqing Li,^{‡ a} Lanlan Chen,^{*a} Lihong Song,^b Xueqiang Zhang,^b
Hongqi Huo,^b Zhixin You,^b Ying Wu,^a Zongsheng Wu,^a Jiamin Ye,^a Qinrui Fu,^a
Lichao Su,^a Xuan Zhang,^a Huanghao Yang,^a and Jibin Song^{*a}

*a MOE key Laboratory for Analytical Science of Food Safety and Biology,
College of Chemistry, Fuzhou University, Fuzhou 350108, China*

*b Department of Nuclear Medicine, Han Dan Central Hospital, Handan, Hebei,
056001, P. R. China*

E-mail: llchen@fzu.edu.cn; jibinsong@fzu.edu.cn

Experimental Section

Materials

Hexadecyltrimethylammonium bromide (C₁₆TAB, >95%), sodium borohydride (NaBH₄, 99%), hydrogen tetrachloroaurate trihydrate (HAuCl₄•3H₂O, 99.995% trace metals basis (Aldrich)), silver nitrate (AgNO₃, >99.97%), hydroquinone (99%), 2,2'-

azino-bis (3ethylbenzothiazoline-6-sulfonic acid) (ABTS), tetraethyl orthosilicate (TEOS, 99.999%), 4-mercaptophenylacetic acid (4-MPAA, 97%), poly(ethylene glycol) and SH-bis(carboxymethyl) ether (SH-PEG-SH, 5000 kDa) were purchased from Sigma-Aldrich. Dihydrochloride (AIPH, 98%) and $TiCl_3$ (15% with 2 M HCl) were purchased from Aladdin. Polyacrylic acid (PAA, $M_w=5,000$) were purchased from J&K Chemical Ltd. NaOH (AR), ammonium hydroxide (AR), ethanol (AR), 2-propanol (AR) were purchased from Sinopharm Chemical Reagent Co., Ltd (Shanghai, China). Sodium bicarbonate ($NaHCO_3$, 99%) and methylene blue (MB, >98%) were purchased from Sinopharm Chemical Reagent Co.,Ltd. DMEM culture medium and Fetal bovine serum (FBS) was purchased from HyClone Inc. Fluorescein PEG Thiol (FITC-PEG-SH) was purchased from Aladdin Chemical Reagent Co., Ltd. Dichlorofluorescein diacetate (DCFH-DA) and HOE33342, Calcein-AM and propidium iodide (PI) Live/Dead double-staining kits, Lyso-Tracker Red and Cell Counting Kit-8 (CCK-8) was supplied by Beyotime Biotechnology (Shanghai, China). 5, 5'-dithiobis (2-nitrobenzoic acid) (DTNB) was purchased from Alfa Aesar. All chemicals were used as received without further purification. Ultrapure water was obtained from a MilliQ water purification system (18.2 MU resistivity, Millipore).

Apparatus

Transmission electron microscopy (TEM) images were collected by a Hitachi-7700 microscope with an accelerating voltage of 100 kV. The FEI Tecnai F20 microscope with accelerating voltage of 200 kV was used to obtain High-angle annular dark-field

scanning transmission electron microscopy (HAADF-STEM) images and elemental mapping. Dynamic light scattering (DLS) was performed on a Zetasizer Nano ZS instrument (Malvern, England). Ultraviolet-visible-near infrared light (UV-Vis-NIR) absorption spectra were recorded using an SH-1000 Lab microplate reader (Corona Electric, Ibaraki, Japan). The confocal laser scanning microscopy (CLSM) imaging was obtained from Nikon A1 (Tokyo, Japan). The Vevo LAZR-X 3100 PA Imaging System (Fujifilm Visual Sonics Co. Ltd, Toronto, Canada) was employed to obtain photoacoustic imaging and ultrasound imaging data *in vitro* and *in vivo*.

Synthesis of Au NRs: The Au NRs were synthesized with minor modification according to a previous work.^[1] The first step was to prepare Au seeds. 4 mg of NaBH₄ and 4 mg of NaOH was dissolved in 10 mL of cold water. **Note that NaBH₄ must be weighed accurately because the concentration of NaBH₄ determines the quality of Au seed.** Then, 100 µL of gold (III) chloride trihydrate (HAuCl₄·3H₂O) (50.8 mM) was dropped into 10 mL of CTAB (0.1 M) aqueous solution under stirring. Subsequently, 460 µL of the mixed solution (NaBH₄ and NaOH) was added into the above solution quickly under vigorous stirring. The Au seed solution was aged for 30 min before use. **The fabrication and aging process of Au seed should be in dark conditions.**

The second step was the growth of Au NRs. 600 µL of Au seed solution was quickly added into the growth solution containing CTAB (50 mL, 0.1 M), HAuCl₄·3H₂O (500 µL, 50.8 mM), AgNO₃ (350 µL, 0.1 M) and hydroquinone (2.5

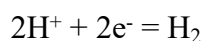
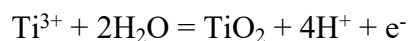
mL, 0.1 M) at 30 °C. Then the reaction was carried out overnight. The Au NRs were collected by centrifugation (11000 rpm, 10 min) and washed twice using deionized water. Finally, the obtained Au NRs were redispersed in 50 mL of deionized water and stored at 4 °C. **Additionally, all the chemicals and reagent should be fresh and pure, especially for HAuCl₄·3H₂O, NaBH₄ and CTAB. Temperature control must be accurate during the Au NRs fabrication process.**

Synthesis of Janus AuNR-TiO₂ nanomotors: The first step was to prepare Janus AuNR-SiO₂ according a previous work.^[2] In detail, 6 mL of the above Au NR dispersions was added to 30 mL of isopropanol (IPA) under vigorous stirring. Afterward, 240 µL of 4-MPAA ethanol solution (0.645 mM) and 720 µL of PAA aqueous solution (5 mM) were added to the mixed solution. After reaction for 45 min, 9 mL of TEOS (8.9 mM) and 1 mL of ammonia were sequentially added to the system. Then, the mixture was reacted for 5 h under stirring at room temperature. **The Janus AuNR-SiO₂ NPs were collected by centrifugation (10000 rpm, 10 min) and washed three times by deionized water to remove residual ammonia, avoiding the effect of residual ammonia on the hydrolysis of TiCl₃. Additionally, the feed ratio of PAA and 4-MPAA is very important. According to the used concentration of Au NRs, the feed ratio of PAA and 4-MPAA should be adjusted accordingly.**

The second step was to deposit TiO₂ on the surface of Au NRs. Typically, 30 µL of TiCl₃ (15%) was added to 5 mL of degassed deionized water under vigorous stirring.

Subsequently, approximately 0.2 mL of NaHCO₃ (1 M) was dropped into the above solution (Note: the required amount of NaHCO₃ might vary slightly according to the difference of TiCl₃' vendors or batches). As the mixed solution became dark blue, the Janus AuNR-SiO₂ NPs were added quickly. The dispersion was then gently kept stirring/shaking for 30 min. The product was collected by centrifuge at 5500 rpm for 8 min and washed with DI water twice. Finally, the Janus AuNR-SiO₂-TiO₂ NPs were obtained.

The hydrolysis of Ti³⁺ follows this process:



The Janus AuNR-TiO₂ nanomotors could be obtained by etching SiO₂ of AuNR-SiO₂-TiO₂ NPs with ammonia. We could obtain AuNR-SiO₂ NPs with various coverage percentage of SiO₂ by adjusting the addition of 4-MPAA. For example, when the addition of 4-MPAA was reduced, the coverage of SiO₂ on the Au NRs dramatically decreased, while the coverage of TiO₂ increased proportionately. Continuing to reduce the addition of 4-MPAA (5 mM) to 140 μL, the obtained AuNR-TiO₂ nanostructures showed gourd-like morphology probably because a small amount of SiO₂ deposited on the surface of Au NRs could be etched by NaHCO₃ during the formation of TiO₂ NPs. In particular, when only PAA was added to the system, the product showed core/shell AuNR-TiO₂ nanostructures.

FDTD calculations: Herein, to confirm the spatial electric field distribution of the AuNR-TiO₂ nanomotors under the irradiation of a beam of linearly polarized light, the finite-difference-time-domain (FDTD) simulation (8.11.337 version, Lumerical Solutions, Inc.) was performed as an effective approach. The refractive index of Au component was adopted from the refractive index database in the simulation software package Gold (Au) -CRC. The refractive index of TiO₂ was adopted from the previous work^[3]. All geometric parameters for the simulation were consistent with the average actual size of as-prepared samples shown in TEM image (Figure 1). In detail, the diameter and length of Au NRs were set as 16 nm and 93 nm, respectively. For the detailed FDTD parameter setting, the simulation region was set as a unit 1200 nm × 800 nm × 800 nm in 3Ds. Herein, boundary conditions were set as perfectly matched layers (PML) in all simulations. To save computational resources while improving computational accuracy, a refined mesh grid near the structure was set as 0.6 nm in a 3D dimension 200 nm × 150 nm × 150 nm. Total-field scattered-field (TFSF) linearly polarized light waves, which was polarized in line with X-axis with a wavelength range of 400-1100 nm, were injected into the unit cell along the -Z direction. The initial amplitude of the electric field vector of the TFSF linearly polarized light vector was set to be 1 V m⁻¹. Two frequency-domain field profile monitors localized at Z=0 nm in the x-y plane and Y=0 nm in the x-z plane for AuNR-TiO₂ NPs, respectively. All frequency-domain field profile monitors were utilized to collect field profile data ($|E/E_0|^2$) of the selected section of target structures while keeping the excitation wavelength 660 nm.

Photocatalytic H₂ generation: All glassware was washed with deionized water before use. The mixture of 1 mg of AuNR-TiO₂ nanomotors, 20 mL of deionized water with 20 μmol of lactic acid was added to a 55 mL of cylinder-shape quartz reactor. NIR laser beam (660 nm, 0.8 W/cm²) was used as light source. Similar to typical photocatalytic experiment, the generated H₂ was monitored by a gas chromatograph (Agilent HP 5890).

Cytotoxicity assay: The cytotoxicity test was carried out using CCK-8 assay. MCF-7 and LO2 cells were incubated in RPMI-1640 culture medium, and MC38 cells were incubated in DMEM culture medium. In detail, three kinds of cells were seeded in 96-well plates (10⁴ cells per well) and cultured for 24 h prior to the experiment. PBS and Au NR-TiO₂ nanomotor PBS dispersions with different concentrations were added to incubate with cells for 24 h. As for the nanomotor + X-ray group, after the cells were incubated with nanomotors for 12 hours, the cells were exposed to X-ray irradiation (the applied X-ray dose was 4 Gy, the irradiation time was 12 min, and the power of the X-ray was 4 W). After 10 h, the CCK-8 assay was carried out. As for the NIR+X-ray irradiation group, after cells were incubated with nanomotors for 12 hours, the cells were irradiated with NIR light first (the applied NIR laser was 0.8 W/cm², each NIR irradiation was 8 min, the rounds of NIR irradiation were 3, and the interval was 20 min), and then exposed to X-ray irradiation. Subsequently, the CCK-8 assay was carried out.

Intracellular ROS detection: Herein, DCFH-DA was used to detect intracellular ROS. Firstly, MCF-7 cells were incubated with nanomotors (80 $\mu\text{g}/\text{mL}$) at 37 $^{\circ}\text{C}$ for 12 h in confocal dish. Then, 800 μL of HOE33342 was added to the cell medium and incubated for 25 min. The cells were washed twice by PBS. Subsequently, 10 mM of DCFH-DA was added to the cells medium and incubated for 30 min. As for the X-ray group, X-ray was used to illuminate the confocal dish (the applied X-ray dose was 4 Gy, the irradiation time was 12 min, and the power of the X-ray was 4 W). As for the NIR+X-ray group, 660 nm laser beam was used to irradiate the cells first (the applied NIR laser beam was 0.8 W/cm^2 , each irradiation time was 8 min, the rounds of irradiation were 3, and the interval was 20 min), and then X-ray was used to illuminate the confocal dish. Finally, the well plates were imaged by a Nikon A1 confocal laser scanning microscope.

Cell cloning experiment: Viable MCF-7 cells were placed in a 6-well plate (1000 cells per well). Then, six groups (n=4 per group) were divided: (1) PBS, (2) NIR, (3) X-ray, (4) nanomotor + NIR, (5) nanomotor + X-ray and (6) nanomotor + NIR + X-ray. The cells were fixed with methanol and stained with 0.5% Gentian Violet after treatment for 8 d. Colonies containing more than 50 cells were counted and the cell clonal formation rate was calculated.

Penetration ability of the nanomotors in cells and their cellular uptake analysis:

MCF-7 cells (1×10^5 cells/mL) were seeded in a confocal dish and cultured for 24 h. Afterward, 50 μ L of nanomotors (4 mg/mL) marked with FITC-PEG-SH were added to the dish. Cells were incubated with nanomotors for 2 h. During the incubation, different rounds of NIR irradiation were carried out. Subsequently, the cells were washed with PBS and were observed by CLSM. The applied NIR laser was 0.8 W/cm², each NIR irradiation time was 8 min, the rounds of NIR irradiation were 3, and the interval was 20 min.

For the cellular uptake analysis, the process was similar to the above procedure. After NIR irradiation treatments and co-incubation with nanomotors for 2 h, the cells were washed by PBS three times and collected for ICP-MS test. The internalization rate of the nanomotors could be calculated through the Au content.

Penetration ability of the nanomotors in 3D MCSs: According to a previous report, MCF-7 cells with a cell density of approximate 5×10^3 cells per milliliter were seeded in a 96 well plate with agarose hydrogel. After culture for 7 d, MCSs were formed and used to incubated with nanomotors for testing penetration ability. FITC dye (green) served as indicator to mark the nanomotors. The system was treated with or without NIR irradiation for different rounds and then co-incubated for 12 h. After that, the MCSs were washed with PBS and then observed by CLSM. The applied NIR laser was 0.8 W/cm², each NIR irradiation was 8 min, the rounds of NIR irradiation were 4, and the interval was 20 min.

Cell organelle colocalization: Nucleus and lysosome were stained by HOE33342 and Lyso-Tracker Red, showing blue and red fluorescence, respectively. Nanomotors were marked with FITC-PEG-SH, showing green fluorescence. MCF-7 cells (1×10^5 cells/mL) were seeded in confocal dishes, divided into two groups, and cultured for 24 h. Afterward, 50 μ L of nanomotors (4 mg/mL) were added to the dish. Cells were incubated with nanomotors for 2 h. One group was treated with NIR laser irradiation for three rounds. Another group was without treatment. Subsequently, these two groups were washed with PBS and were observed by CLSM. The power density of the applied NIR laser was 0.8 W/cm^2 , each exposure time was 8 min, and the interval was 20 min.

Abiotic detection of glutathione: The radio-induced depletion ability of different samples to glutathione (GSH) was detected by the Ellman's assay. In detail, Au NPs, TiO₂ NPs and Au-TiO₂ nanomotors (1 mL, 80 μ g/mL) were mixed with GSH solution (0.5 mL, 10 mM), respectively, under stirring for 10 min. Subsequently, each group was irradiated with or without X-ray for 12 min (X-ray: 50kV, 80 μ A). After 30 min, Tris-HCl buffer (50 mM, pH=8.8) and bicarbonate buffer solution (50 mM, pH = 8.8) containing DTNB (100 mM) were sequentially added under gently shaking and then incubated for 10 min in the dark. Finally, an SH-1000 Lab microplate reader was used to collect the absorption at 410 nm.

Animal experiments: All the animal experimental procedures were in accord with the guidelines of the Regional Ethics Committee for Animal Experiments and the Care Regulations approved by the Institutional Animal Care and Use Committee of Fuzhou University.

Establishment of subcutaneous tumor mice model: All female nude BALB/c mice (about 20 g) were supplied by WuShi, Inc. (Shanghai, China). Typically, subcutaneous tumor mice models were established by subcutaneously injecting of 100 μL and 1×10^7 of MCF-7 cell suspension into the right back of mice.

Establishment of orthotopic liver cancer mice model: 25 μL and 1×10^7 of MC38-luc cells were directly injected into the liver of the male nude mice exposed through the incised skin, and then the wound was sutured immediately with anti-inflammatory treatment.

***In vivo* PAI and USI measurements:** MCF-7-tumor-bearing mice were used to study the *in vivo* tumoral biodistribution of nanomotors. Vevo LAZR-X 3100 PA Imaging System was used to record the tumor-bearing mice after intravenous injection of nanomotors at fixed time point and monitor the movement behavior of nanomotors driven by NIR laser irradiation (excitation at 1250 nm).

***In vivo* bioluminescent imaging:** By injecting luciferin potassium salt, the bioluminescent imaging of MC38 orthotopic liver cancer can be achieved using IVIS® Lumina XRMS Series III small animal imager to monitor the growth of liver cancer. When the fluorescence intensity of tumor reached to 5×10^3 p/sec/cm²/sr, 100 μ L of AuNR-TiO₂ PBS dispersions (4 mg/mL) were intravenously injected. Photoacoustic imaging was carried out using a Visual Sonic Vevo 3100 LAZR system.

Histology Studies: The mice of each group were euthanized after treatments under different conditions. The heart, liver, spleen, lung, kidneys and tumor tissues from tumor-bearing mice were collected and soaked in 4% paraformaldehyde solution. After embedded and sectioned, the major organs and tumor tissues of each group were measured by hematoxylin and eosin (H&E) staining assay.

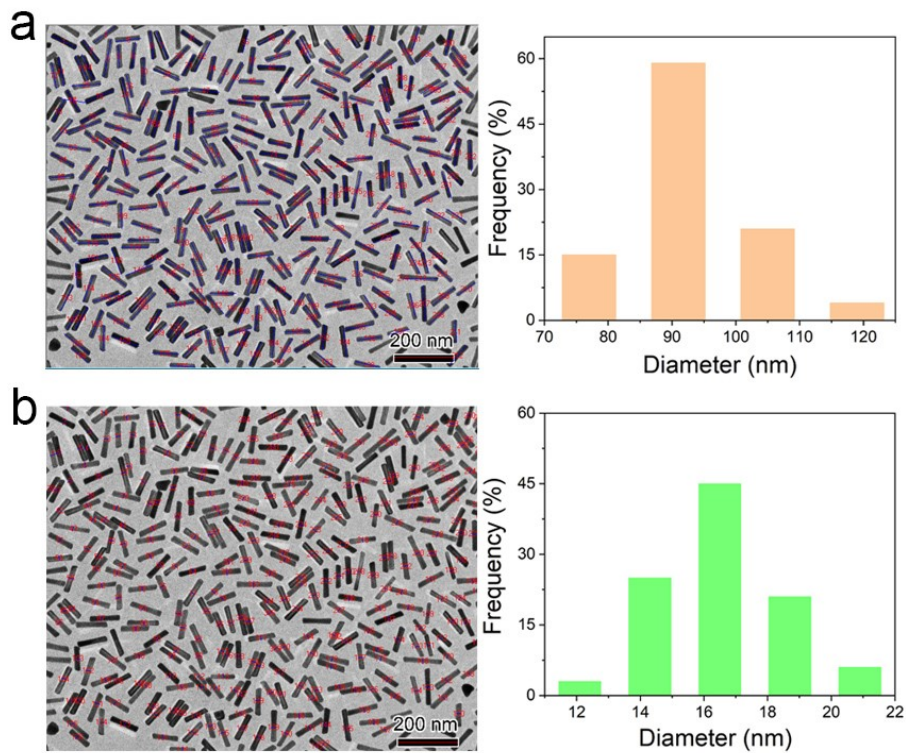


Figure S1. The statistical results of Au NRs in (a) length and in (b) outer diameter analyzed with Nano Measure 1.2.

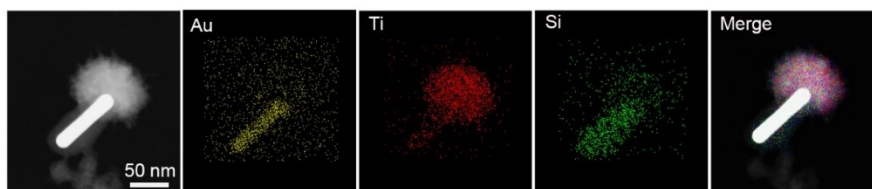


Figure S2. High-angle annular dark-field (HAADF) image of an AuNR-SiO₂-TiO₂ nanostructure and corresponding element mapping.

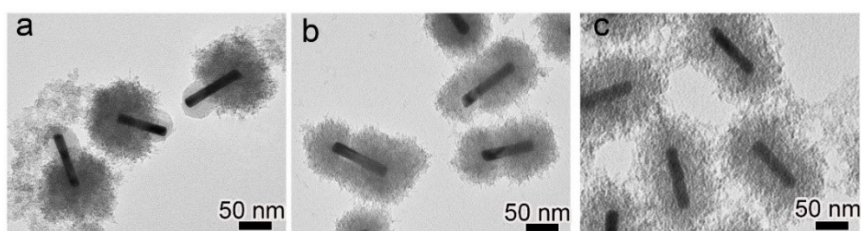


Figure S3. TEM images of AuNR-TiO₂ nanostructures with different morphologies by adjusting the addition of 4-MPAA: (a) 180 μL, (b) 140 μL and (c) 0 μL of 4-MPAA. Note that we obtained gourd-like AuNR-TiO₂ composite as the 4-MPAA was reduced to 140 μL.

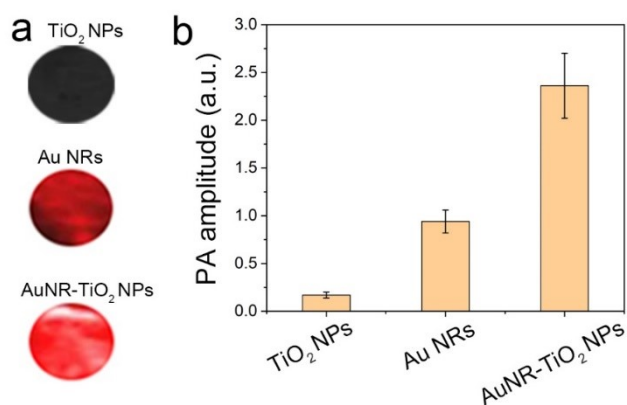


Figure S4. (a) PAI photographs and (b) corresponding PAI intensity of different samples (1 mg/mL of TiO₂ NPs, 1 mg/mL of Au NRs, and AuNR-TiO₂ NPs prepared with 1 mg/mL of Au NRs).

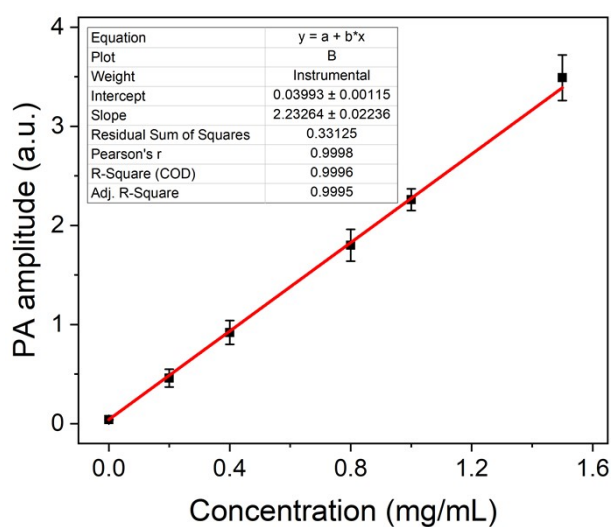


Figure S5. The PAI intensity of the nanomotors vs. the concentration.

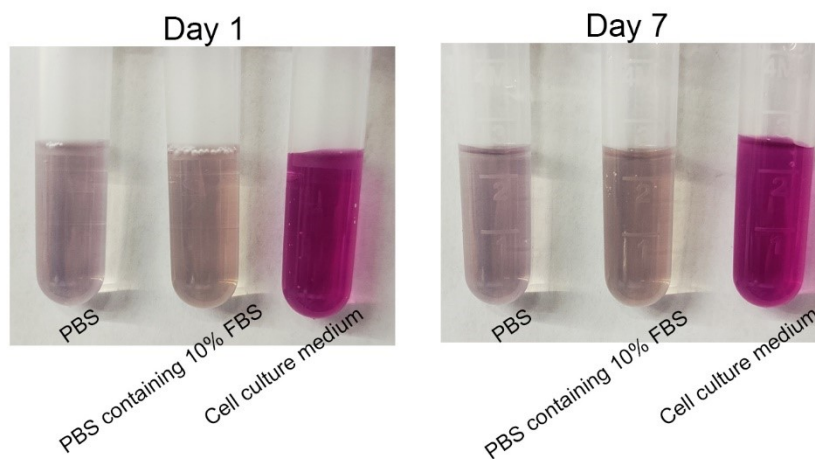


Figure S6. Photographs of the AuNR-TiO₂ nanomotors in physiological mimicking conditions on day 1 and day 7.

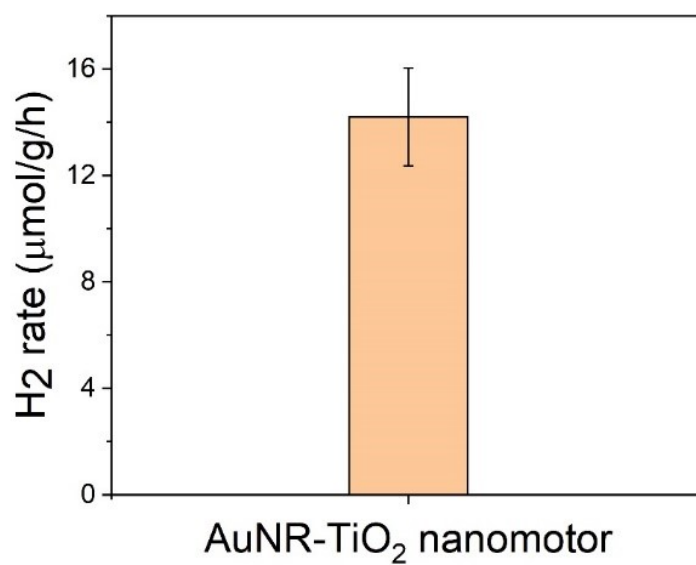


Figure S7. H₂ evolution rate of AuNR-TiO₂ nanomotors under NIR laser irradiation (laser power: 0.8 W/cm²).

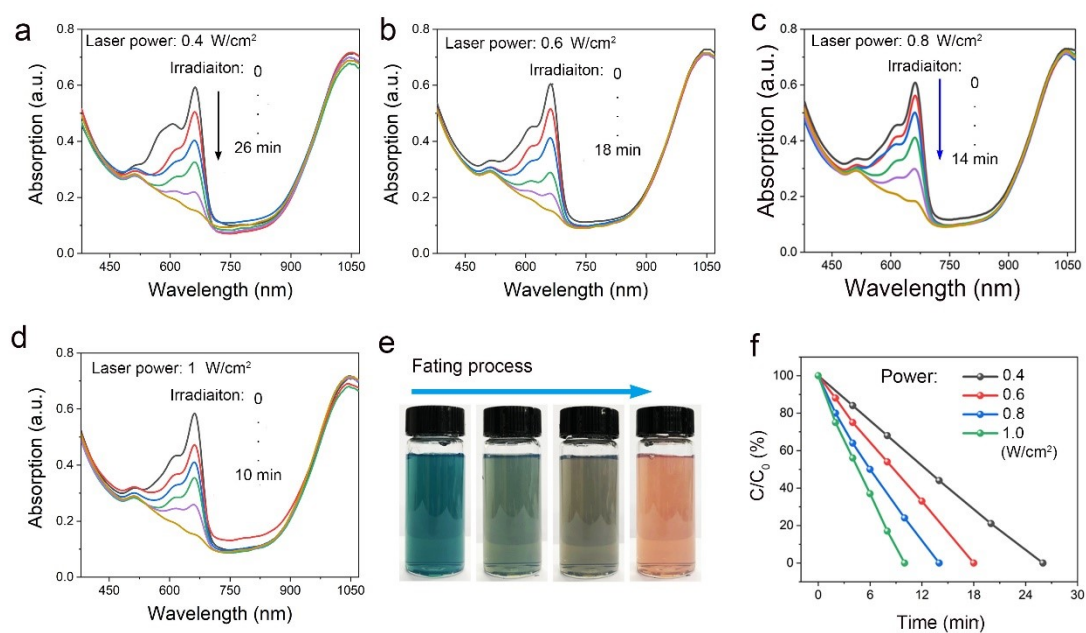


Figure S8. (a-d) UV-vis-NIR spectra of the AuNR-TiO₂ nanomotor/MB aqueous solution system in the de-coloration process upon NIR laser irradiation with different power: (a) 0.4, (b) 0.6, (c) 0.8 and (d) 1.0 W/cm². (e) Digital photographs of the de-coloration process. (f) De-coloration rate of the AuNR-TiO₂ nanomotor/MB aqueous solution system with NIR laser irradiation.

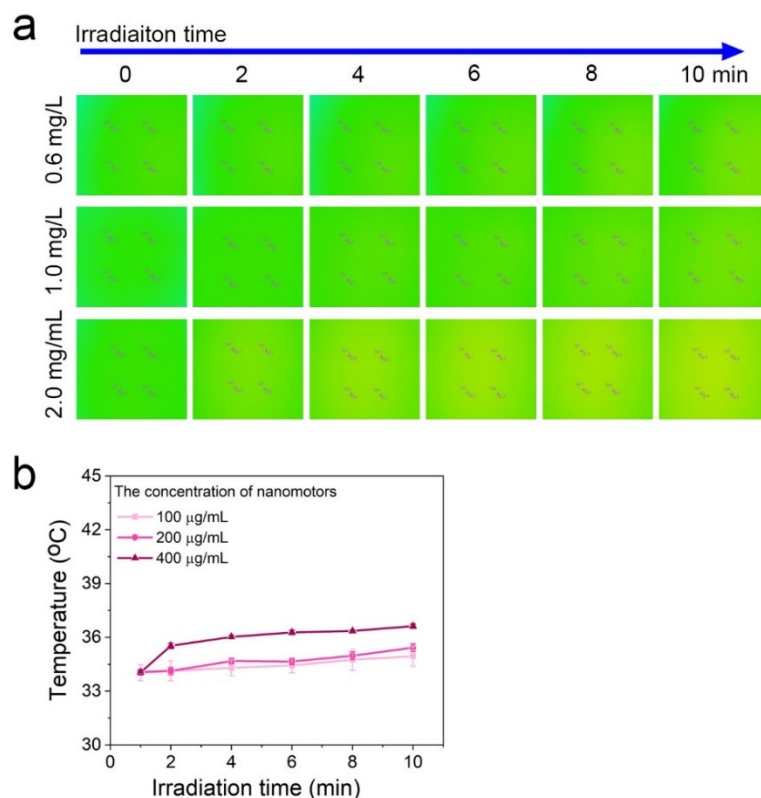


Figure S9. (a) IR thermal images of AuNR-TiO₂ nanomotors with different concentration and (b) their changing curves of the temperature as a function of irradiation time.

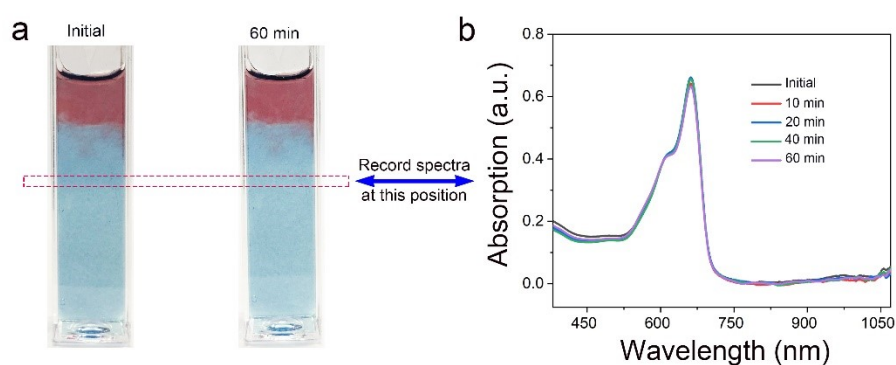


Figure S10. (a) Digital photographs and (b) UV-Vis-NIR absorption spectra of AuNR-TiO₂ nanomotors in agarose hydrogel (0.05 wt%) at a distance of 8 mm from the starting position without NIR laser irradiation.

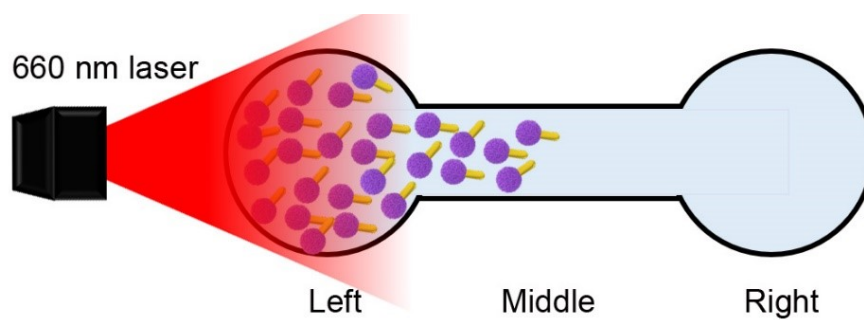


Figure S11. Schematic illustration showing the movement behavior of AuNR-TiO₂ nanomotors triggered by NIR laser in a two-outlet microfluid channel.

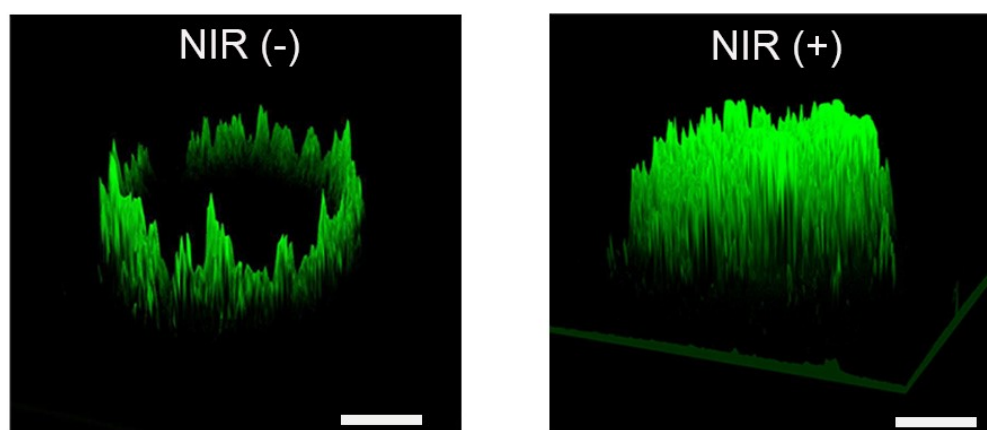


Figure S12. The 3D model of the nanomotor distribution in 3D MCSs at the scanning depth of 120 μm .

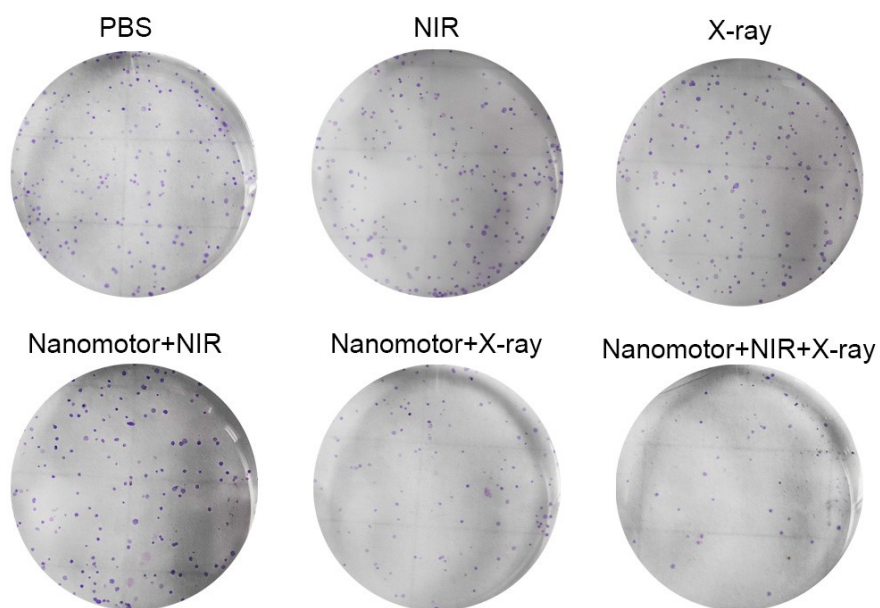


Figure S13. Photographs of the cell clonal formation with different treatments.

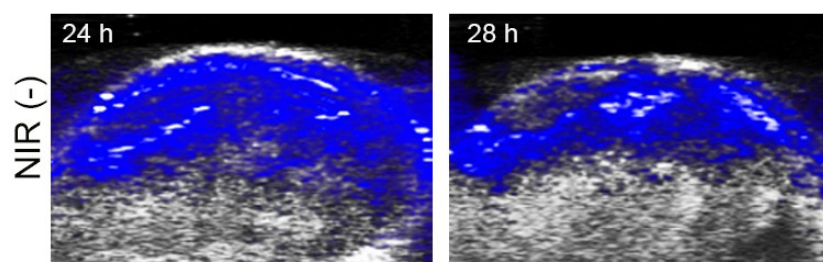


Figure S14. *In vivo* NIR-II PA images after intravenous injection of nanomotors.

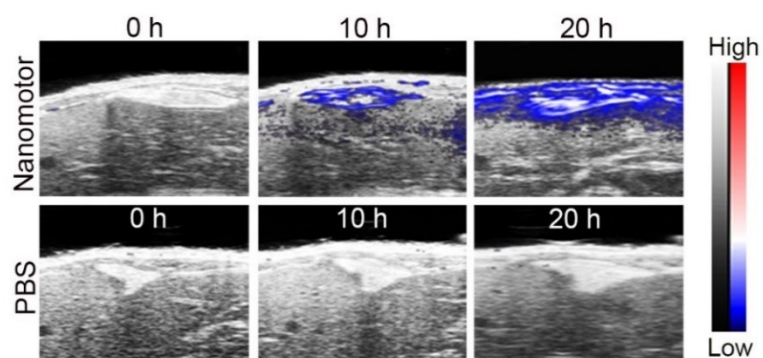


Figure S15. *In vivo* NIR-II PA images in different groups in orthotopic liver models after intravenous injection of PBS and nanomotors, respectively (excitation at 1250

nm).

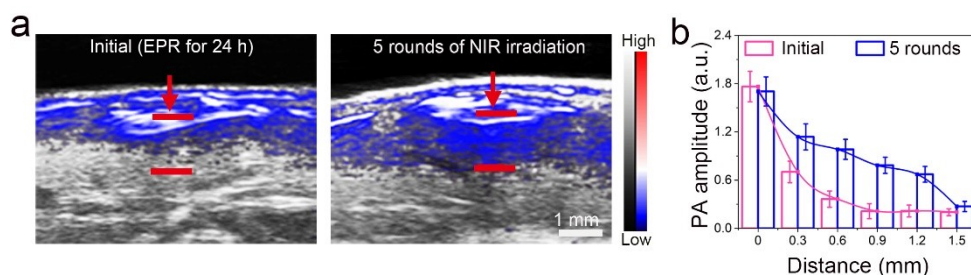


Figure S16. (a) Representative 2D PA images in the orthotopic liver cancer model before and after NIR irradiation, and (b) the histogram of PA intensity vs. penetration depth.

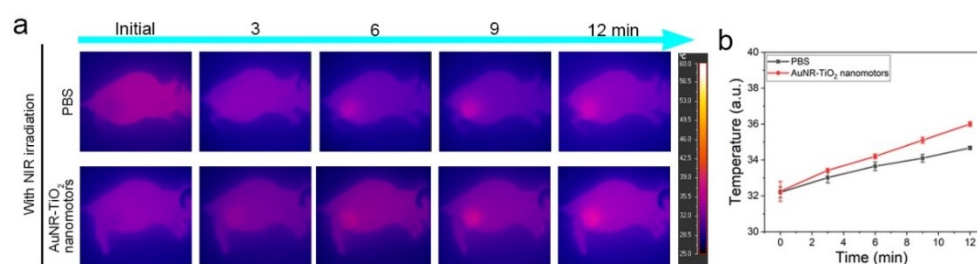


Figure S17. (a) IR thermal images of MCF-7-tumor-bearing mice with intravenous injection of PSB and AuNR-TiO₂ nanomotors, respectively, under the NIR laser irradiation, and (b) the corresponding changing curves of local temperature at the tumor area vs. irradiation time (laser power = 0.8 w/cm²).

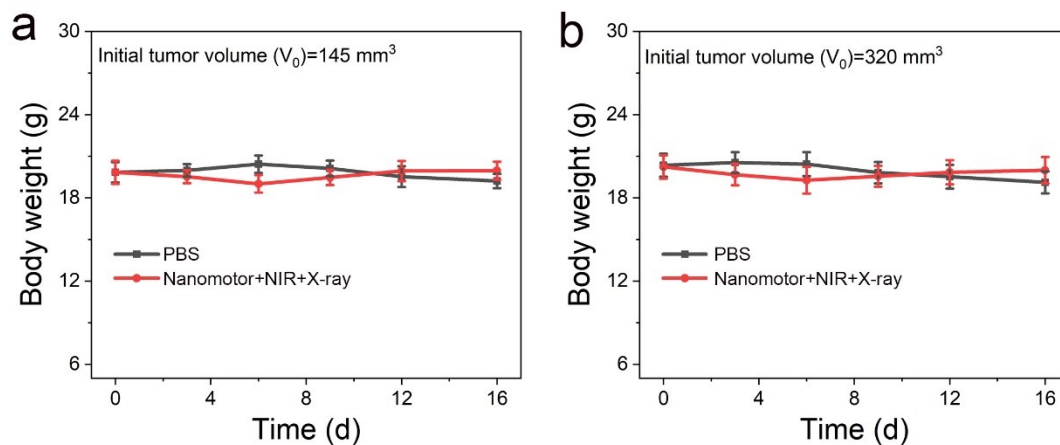


Figure S18. Body weight of MCF-7-tumor-bearing mice with initial tumor volume of (a) 145 mm³ and (b) 320 mm³ as a function of time.

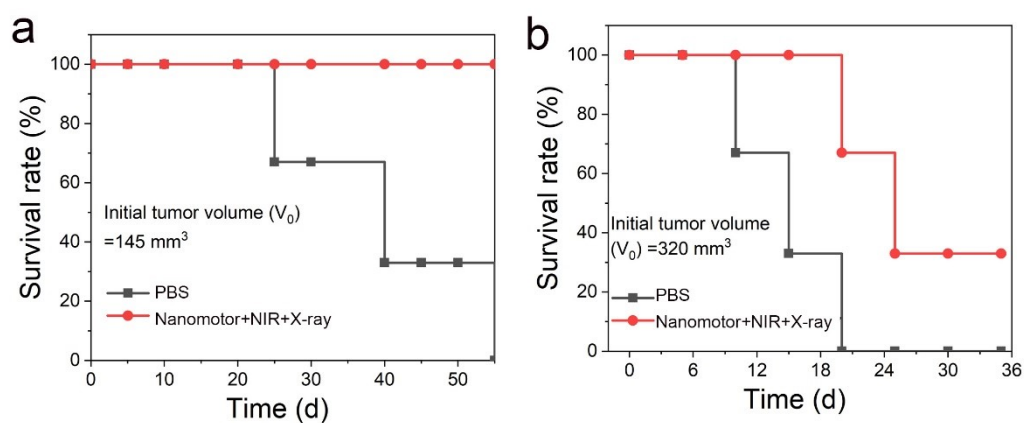


Figure S19. Survival rate of MCF-7-tumor-bearing mice with initial tumor volume of (a) 145 mm³ and (b) 320 mm³ as a function of time.

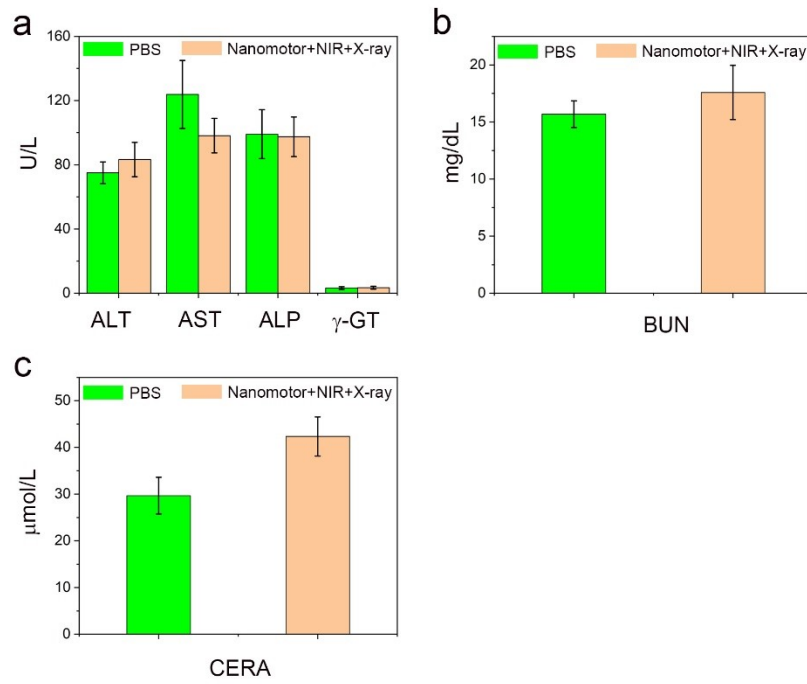


Figure S20. Blood biochemical analysis of subcutaneous tumor-bearing mice after different treatments including liver and kidney functions: alkaline phosphatase (ALP), alanine transaminase (ALT), aspartate transaminase (AST), γ -glutamyl transpeptidase (γ -GT), blood urea nitrogen (BUN), creatinine (CREA) (n =3).

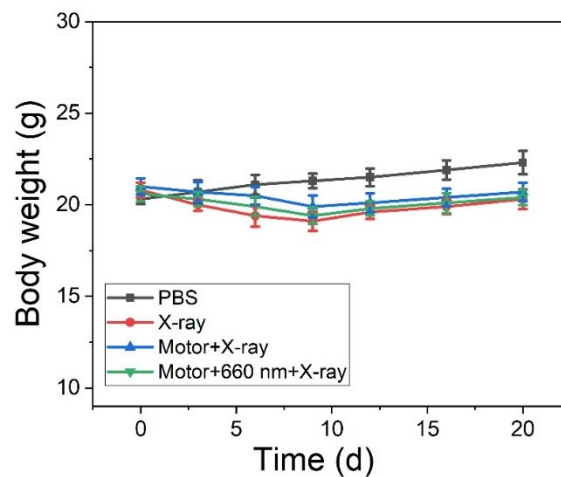


Figure S21. Body weight of orthotopic liver tumor-bearing mice with different treatments vs. time.

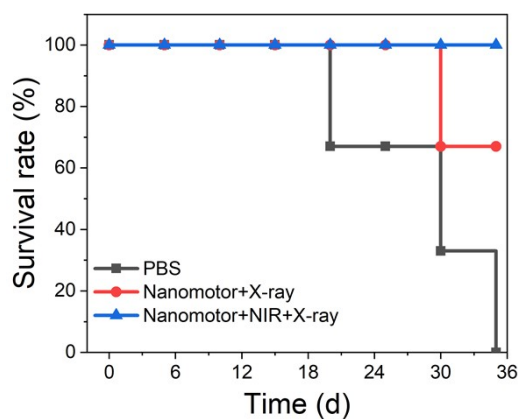


Figure S22. Survival rate of orthotopic liver tumor-bearing mice with different treatments vs. time.

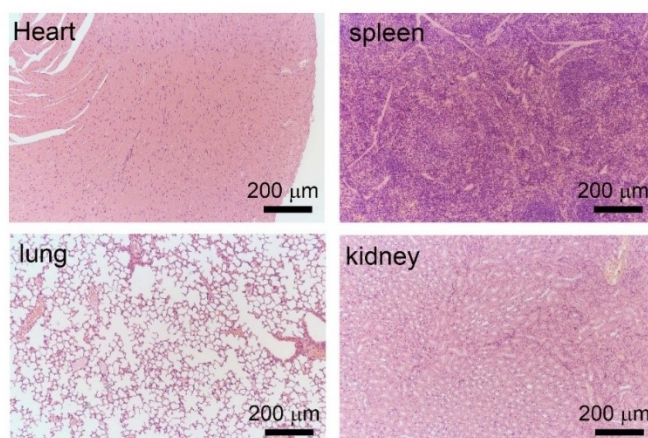


Figure S23. Histological examination of main organs (heart, liver, spleen, lung and kidney) from orthotopic live tumor-bearing mice in the nanomotors + NIR + X-ray group.

References:

- [1] L. Vigderman, E. R. Zubarev, *Chem. Mater.* **2013**, *25*, 1450-1457.
- [2] T. Chen, G. Chen, S. Xing, T. Wu, H. Chen, *Chem. Mater.* **2010**, *22*, 3826-3828.
- [3] S. Sarkar, V. Gupta, M. Kumar, J. Schubert, P. T. Probst, J. Joseph, T. A. F. König, *ACS Appl. Mater. Interfaces* **2019**, *11*, 13752-13760.